Selective Complexation and Transport of Europium Ions at the Interface of Vesicles

Valérie Marchi-Artzner,*[a, c] Marie-Josephe Brienne,[a] Thaddée Gulik-Krzywicki,[b] Jean-Claude Dedieu,[b] and Jean-Marie Lehn*[a]

Abstract: The aim of the present work was to design functionalized lipidic membranes that can selectively interact with lanthanide ions at the interface and to exploit the interaction between membranes induced by this molecular-recognition process with a view to building up self-assembled vesicles or controlling the permeability of the membrane to lanthanide ions. Amphiphilic molecules bearing a β-diketone unit as head group were synthesized and incorporated into phospholipidic vesicles. Binding of Eu^{III} ions to the amphiphilic ligand can lead to formation of a complex involving ligands of the same vesicle membrane (intravesicular complex) or of two different vesicles (intervesicular complex). The effect of Eu^{III} ions on vesicle behavior was studied by complementary techniques such as fluorimetry, light scattering, and electron microscopy. The formation of an intravesicular luminescent Eu/β-diketone ligand (1/2) complex was demonstrated. The linear increase in the binding constant with increasing concentration of ligands in the membrane revealed a cooperative effect of the ligands distributed in the vesicle membrane. The luminescence of this complex can be exploited to monitor the kinetics of complexation at the interface of the vesicles, as well as ion transport across the membrane. By encapsulation of 2,6-dipicolinic acid (DPA) as a competing ligand which forms a luminescent Eu/DPA complex, the kinetics of ion transport across the membrane could be followed. These functional vesicles were shown to be an efficient system for the selective transport of Eu^{III} ions across a membrane with assistance by β-diketone ligands.

Keywords: ion transport · lanthanides · ligand design · lipids · vesicles

Introduction

Molecular recognition of metal ions at the interface of a lipidic membrane can be the first step of ion transport through biological membranes, as is observed in biological cells. For example, the binding of divalent calcium ions to phosphatidylcholine lipids is of great importance in a biological context.[1] The activity of numerous membrane proteins involved in cell adhesion, such as cadherins, is dependent on calcium ions. Biological membranes are impermeable to ions,[2] and membrane proteins or peptides modulate ion fluxes across the lipid bilayer. The presence of ions can affect the stability of the membrane and even induce reorganization of the lipids within the membrane[3] or a phase transition, as is observed for phosphatidylethanolamine in the presence of La^{III}.[4] Furthermore, the presence of divalent ions such as Ca^{II} or Mg^{II} induces aggregation or fusion of negatively charged vesicles, while the presence of monovalent ions does not.[5] The addition of lanthanide ions to negatively charged vesicles was also reported to induce such phenomena. Indeed vesicles composed of an anionic phosphate-functionalized lipid effect the permeability to lanthanide ions by forming lipophilic complexes,[6] but the ion selectivity of these systems remains very poor because the interaction is essentially electrostatic.[7] To improve the ion selectivity, amphiphilic derivatives of β-diketone ligands were chosen in view of their ability to bind lanthanides and to form stable luminescent complexes with Eu^{III} ions.[8]

We describe here the preparation of functionalized vesicles bearing at the interface β-diketone groups that can selectively bind lanthanide ions. Our objective was to explore whether metal/ligand molecular recognition can be used as a tool to build up functional artificial membranes that can be tuned for ion transport or for inducing controlled formation

[a] Dr. V. Marchi-Artzner, Dr. M.-J. Brienne, Prof. Dr. J.-M. Lehn
Laboratoire de Chimie des Interactions Moléculaires
CNRS UPR 285, Collège de France
11 Place Marcelin Berthelot, 75231 Paris cedex 05 (France)
E-mail: valerie.marchi-artzner@univ-rennes1.fr
jean-marie.lehn@college-de-france.fr

[b] Dr. T. Gulik-Krzywicki, Dr. J.-C. Dedieu
Centre de Génétique Moléculaire, CNRS 91198
Gif-sur-Yvette (France)

[c] Dr. V. Marchi-Artzner
Present address: SESO UMR 6510, Université de Beaulieu, Rennes 1
263 Avenue du Général Leclerc, 35042 Rennes Cedex (France)
E-mail: valerie.marchi-artzner@univ-rennes1.fr

DOI: 10.1002/chem.200305423

of self-assembled membranes of vesicles, as in the case of recosomes.[9–12]

We synthetized amphiphilic β-diketone ligands composed of a lipidic anchor, a hydrophilic poly(ethylene glycol) spacer, and a ligand head group (Scheme 1). The complexation of lanthanides ions at the interface of vesicles decorated with ligand **L** (**5a**) and the interaction between such vesicles in the presence of lanthanide ions were analyzed by fluorimetry, dynamic light scattering, and electron microscopy. The Eu^{III}/β-diketone ligand complex exhibited strong luminescence due to energy transfer from the ligand to the lanthanide ions with high efficiency.[13] This property has been used for sensitive detection of Eu^{III} complexation in vesicle suspensions.[14]

The ability of ligand **L** to transport Eu^{III} ions across the membrane and the kinetics of this transport were also studied by using a fluorescence permeability test. Such functional vesicles that can entrap lanthanide ions in the aqueous internal compartment of the vesicle have potential applications in extracting lanthanides from aqueous solutions, for labeling therapeutic vectors, in magnetic resonance imaging[15,16] and for staining biomolecular systems.[8]

Results and Discussion

Synthesis of the amphiphilic β-diketone ligands 5a and 5b: The amphiphilic compounds **5** bearing a β-diketone as head group, two hexadecyl chains as lipophilic anchor, and two hydrophilic tetra- or hexaethyleneoxy spacers were synthesized according to Scheme 1. Commercial monoethers **1** of

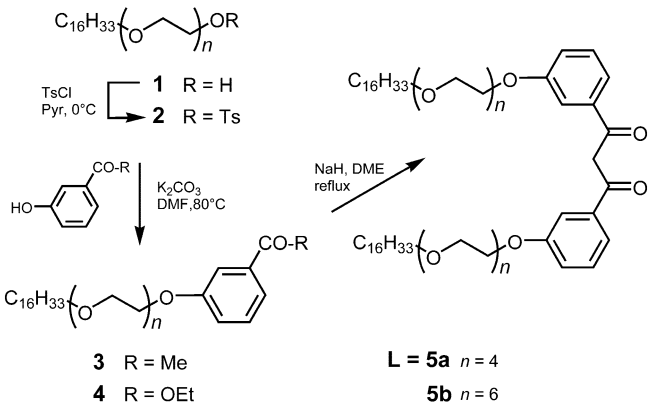

Scheme 1. Synthesis of the β-diketones **5a** and **5b**.

tetra- and hexaethylene glycol were treated with tosyl chloride in pyridine. The resulting tosylates **2** were condensed with *m*-hydroxyacetophenone and ethyl *m*-hydroxybenzoate in the presence of K_2CO_3 in DMF to give **3** and **4**, respectively, in 80–90% yield. Treating an equimolar mixture of **3** and **4** with NaH following a literature procedure afforded the desired β-diketones **5** in 20–35% yield.[17] In the following, only the behavior of compound **5a**, named ligand **L**, will be described.

Complexation of Eu^{III} ions by β-diketone amphiphile L in solution: To test the ability of **L** to chelate Eu^{III} in ethanol solution, titration of Eu^{III} by **L** was monitored by UV and fluorescence spectroscopy. The stoichiometry of the **L**/Eu^{III} complex was determined by the Job method in ethanol solution.[18] With both techniques a maximum was observed around 65 mol% of **L**, close to what is expected for a 1/2 complex $Eu\mathbf{L_2}$ (Figure 1). With β-diketono ligands which do

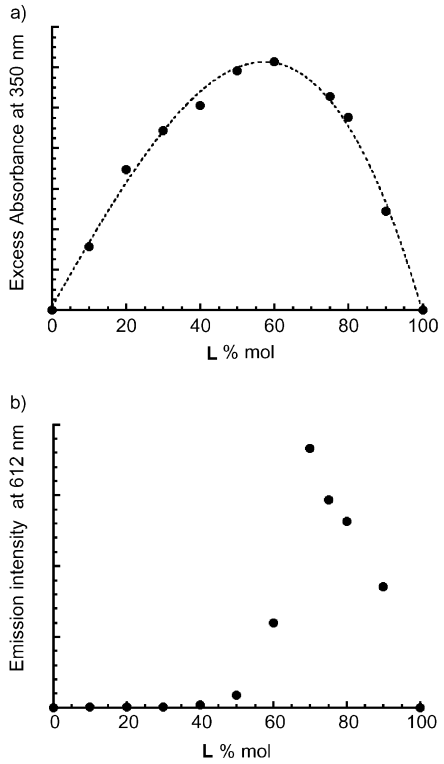

Figure 1. Job diagram of a solution of the lipid **L** (**5a**, 48 μM) and $Eu(NO_3)_3$ in ethanol obtained by a) UV spectroscopy and b) fluorescence spectroscopy with excitation at 350 nm

not have long alkyl chains, octacoordinate chelate complexes of europium were isolated in the solid state.[19] The smaller metal/ligand ratio observed here suggests that other ligands such as ethanol or water may act as additional ligands. On excitation of the ligand **L** at 350 nm, a high-intensity emission was observed at 612 nm, which corresponds to luminescence of the europium ion occurring by an intramolecular energy transfer from the ligand to the europium ion only in the case of the $Eu\mathbf{L_2}$ species. Indeed, the very low fluorescence intensity for 0–50 mol% of ligand means that the initially formed 1/1 species is nonluminescent. Thus, only the $Eu\mathbf{L_2}$ complex is detected by fluorescence spectroscopy.

Preparation of LUVs functionalized by β-diketone L and their stability in the presence of Eu ^{III} ions: Large unilamellar vesicles (LUVs) composed of 0.1–5 mol% of **L** and egg phosphatidylcholine (EPC) as lipid matrix were prepared by the extrusion method. The presence of **L** in the vesicles was checked by observing the UV absorption band of the ligand

at 350 nm after vesicle filtration. Due to the method of vesicle preparation, the ligand was statistically distributed within the two leaflets of the vesicle bilayer.

To evaluate the solubility of the ligand in EPC or dipalmitoyl phosphatidylcholine (DPPC) lipid bilayers, calorimetry was performed on suspensions of multilamellar vesicles composed of different **L**/EPC or **L**/DPPC mixtures, as shown in Figure 2a and b, respectively. We analyzed the solubility in EPC and DPPC lipid matrix to study the effect of the state of the vesicle membrane (gel or fluid) on the complexation process. First, for pure ligand **L**, a peak corresponding to fusion of the hexadecyl chains was observed at 61 °C with $\Delta H = 139\ J\,g^{-1}$, values slightly lower than those obtained for **L** in the solid state. A peak at the same position was observed for a 5/95 **L**/EPC mixture and attributed to the pure ligand **L** (Figure 2a). The ΔH value for this peak of $72\ J\,g^{-1}$, normalized with respect to the amount of **L** in the mixture, is about half the value for pure **L.** For a 3/97 **L**/EPC mixture virtually no peak was observed. These results show that there is no significant segregation of ligand **L** in the EPC bilayer below 3 mol % of **L**. In other words, the ligand **L** is soluble in the EPC bilayer up to about 3 mol %, while at 5 mol % **L** tends to segregate in the membrane. In the case of **L**/DPPC mixtures (Figure 2b), a very small peak corresponding to pure **L** was only detected for 5/95 and 3/97 **L**/DPPC mixtures. On the other hand the peak of DPPC corresponding to the transition from L_α to $L_{\beta'}$ at 41.7 °C and the pretransition between $L_{\beta'}$ and $P_{\beta'}$ around 30 °C were observed for all mixtures, and this suggests that the presence of **L** does not change the state of the DPPC membrane (data not shown).[20] In conclusion **L** appears to be soluble in DPPC lipid membrane up to 5 mol % and thus is more soluble in DPPC than in EPC matrix, as expected from the length of the two hexadecyl chains of **L**, which corresponds to that of DPPC.

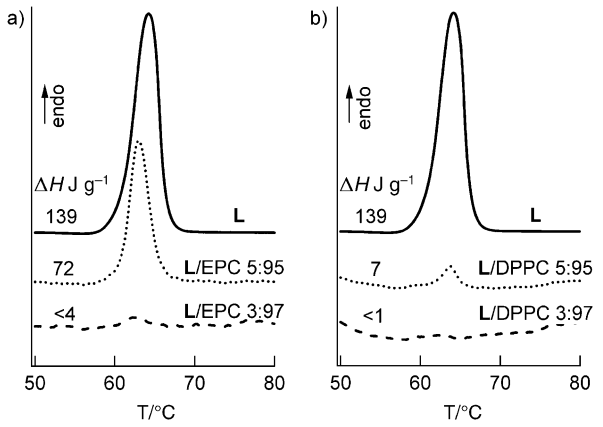

Figure 2. Calorimetric curves of multilamellar vesicle suspensions composed of different mixtures in pure water: a) **L**/EPC; b) **L**/DPPC. The total lipid concentration was fixed at $[lipid] = 100\ mg\,mL^{-1}$. The peaks are normalized with respect to the amount of **L**.

The effect of adding lanthanide ions on vesicle stability and interactions was appraised by determining the change in size and morphology of pure EPC and **L**/EPC LUVs by dynamic light scattering. The results are summarized in Table 1. As expected for preparation by extrusion, the **L**/EPC vesicles had a mean diameter of about 100 nm and were unilamellar, as shown by freeze-fracture electron microscopy.

Table 1. Mean diameters D_n in nm (±20 %) of **L**/EPC or pure EPC LUVs at [lipid] = 0.44 mM in the presence of Eu^{III} at various concentration ratios $[Eu^{III}]/[lipid]$.

mol % of **L**	$[Eu^{III}]/[lipid]$			
in EPC	0	0.023	0.23	2.3
0	100	–	650	–
0.1	90	100	940	100
1	90	–	315	–

The addition of Eu^{III} induced an increase in vesicle size when the ratio $[Eu^{III}]/[lipid]$ of the lanthanide concentration and the total lipid concentration were in the same range (around 0.25) even in the absence of the ligand **L**. No change in size was observed on addition of either a large excess or only a small amount of Eu^{III} relative to the total lipid concentration. To explain the effect of Eu^{III} ions one can consider the electrostatic effect of binding of ions to the vesicle membrane. Europium(III) ions are known to interact with the phosphate head group of lecithin phosphatidylcholine.[21] For example, the adsorption constant of La^{III} ions on the surface of palmitoyl oleyl phosphatidyl glycerol (POPG) or palmitoyl oleyl phosphatidyl choline (POPC) vesicles was determined to be $K_{app} \approx 10^3\ M^{-1}$.[22] Since initially the EPC vesicles were slightly negatively charged,[23] Eu^{III} binding resulted in electrical neutralization of the vesicle surface and thus increased the attractive van der Waals forces between vesicles, which tended to aggregate.[7] These results were confirmed by freeze-fracture electron microscopy (Figure 3).

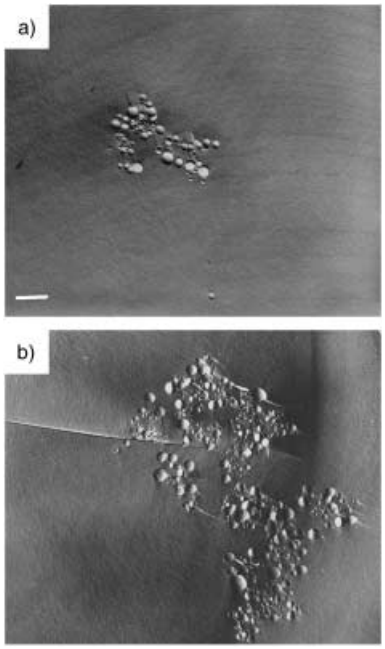

Figure 3. Cryofracture electron microscographs of LUVs ([lipid] = 2.5 mM) in the presence of 0.5 mM $EuCl_3$ ([Eu]/[lipid] = 0.2): a) pure EPC LUVs, b) 0.1 % mol **L**/EPC LUVs. The scale bar represents 200 nm.

In the following, the ratio [Eu]/[lipid] was always less than 0.1, under which conditions the addition of lanthanide ions to EPC vesicles does not induce aggregation. The size of the vesicles prepared by the extrusion method was checked by dynamic light scattering. The question arises whether complexation occurs and, if so, how the lanthanide ions interact with vesicles functionalized by ligand **L**.

Complexation of Eu^{III} ions to L/EPC vesicle membranes: To detect the complexation of the lanthanide ions at the bilayer/water interface of the **L**/EPC vesicles, the effect of adding of Eu^{III} aliquots to a suspension of **L**/EPC vesicles was followed by fluorescence and UV spectroscopy. Beforehand, we checked that an aqueous solution of Eu^{III} salt did not exhibit any fluorescence due to the quenching of the emission of the hydrated Eu^{III} ion by water molecules even in the presence of pure EPC vesicles. On excitation of the β-diketone ligand **L** (350 nm), the addition of Eu^{III} caused a large increase in the emission intensity of Eu^{III}, which eventually reached a plateau (Figure 4).

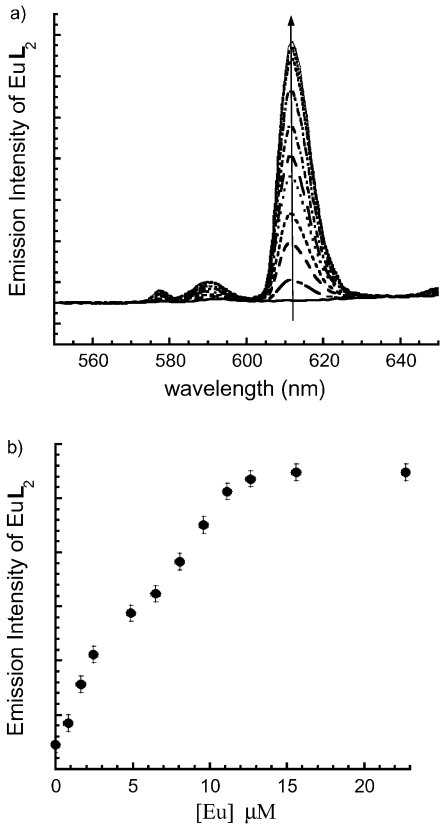

Figure 4. a) Fluorescence spectra of a LUV suspension composed of a **L**/EPC (5/95) mixture (total lipid concentration [lipid] = 0.23 mM) during titration with a solution of $Eu(NO_3)_3$ in a buffer solution containing 10 mM Tris (pH 8). b) Emission fluorescence at 612 nm of the complex Eu$\mathbf{L}_2$ during the titration.

The observed increase in Eu^{III} emission intensity was attributed to energy transfer from the ligand to the metal that occurs only in the Eu$\mathbf{L}_2$ complex, as seen before for experiments in solution. The Eu^{III} ions bind to **L** at the interface of the **L**/EPC vesicles to form a luminescent complex Eu$\mathbf{L}_2$ until all the ligands **L** are complexed at the end of the titration, corresponding to the plateau observed.

To test whether this complexation is a reversible process, we used a strong competitor ligand, namely, 2,6-pyridinedicarboxylic acid (DPA), which is known to form very stable, luminescent complexes with Eu^{III}.[24,25] By direct excitation of either DPA or ligand **L**, one can follow the luminescence of the two complexes formed, $Eu(DPA)_3$ and Eu$\mathbf{L}_2$. At the end of the titration of **L**/EPC vesicles with Eu^{III}, aliquots of DPA were added stepwise. The changes in the emission intensities of the two complexes $Eu(DPA)_3$ and Eu$\mathbf{L}_2$ are shown in Figure 5.

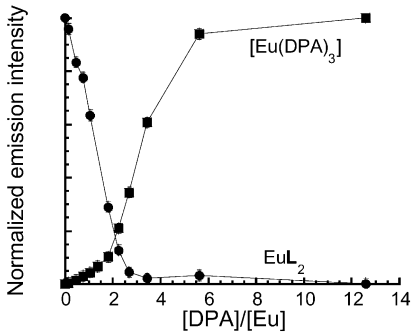

Figure 5. Emission intensities during the titration of a solution of 5% mol **L**/EPC LUVs ([lipid] = 0.29 mM) containing $Eu(NO_3)_3$ (13.4 μM) with a solution of DPA for the Eu$\mathbf{L}_2$ complex (●, excitation at 350 nm) and for $Eu(DPA)_3$ complex (■, excitation at 290 nm)

Initially, all the ligands **L** were complexed to Eu^{III}, so that the normalized emission intensity of Eu$\mathbf{L}_2$ was maximal. During the titration with DPA, the luminescence signal of Eu$\mathbf{L}_2$ decreased, while the emission of $Eu(DPA)_3$ increased and reached a plateau for the addition of three equivalents of DPA. This result is in agreement with an exchange reaction between ligands **L** and DPA that results in complete dissociation of the Eu$\mathbf{L}_2$ complex [Eq. (1)].

$$Eu\mathbf{L}_2 + 3\,DPA \rightleftharpoons Eu(DPA)_3 + 2\,\mathbf{L} \quad (1)$$

Thus the complexation of Eu^{III} on the **L**/EPC vesicle bilayer surface is reversible, and the complexation reaction at the interface of the vesicle is an equilibrium process.

The question is how the organization of the amphiphilic ligands within the membrane affects the complexation. Consider the equilibrium of complexation of Eu^{III} to the ligand **L** with a 1/2 stoichiometry [Eq. (2)].

$$Eu + 2\,\mathbf{L} \rightleftharpoons Eu\mathbf{L}_2 \quad (2)$$

For the whole solution, the apparent binding constant K_{app} is expressed by Equation (3), where the volume concentration of each constituent i is defined as $[i] = n_i/V$, the ratio of the number of moles of i to the total volume V of the solution.

$$K_{app} = \frac{[Eu\mathbf{L}_2]}{[Eu][\mathbf{L}]^2} \quad (3)$$

Assuming that the ligand **L** and the complex $Eu\mathbf{L}_2$ are entirely incorporated into and soluble in the EPC membrane, the binding constant at the interface of the vesicle can be written as Equation (4), where the surface concentration of each constituent i is defined as $(i) = n_i/S$, the ratio of the number of moles of i to the total surface area S of the lipidic bilayer, which can be evaluated from n_{lipid}, the Avogadro number N, and the mean surface area a occupied by one lipid head group (taken to be 0.7 nm^2)[26] according to the relation $S = n_{lipid}aN$.

$$K_a^{bilayer} = \frac{(Eu\mathbf{L}_2)}{[Eu](\mathbf{L})^2} \quad (4)$$

By combining the above relations, the complexation binding can be expressed by Equations (5)–(7) where $\chi_L = n_L/n_{lipid}$, the ratio of the number of moles of **L** to the total number of moles of lipid.

$$K_{app} = K_a^{bilayer}\frac{V}{S} \quad (5)$$

$$K_{app} = \frac{K_a^{bilayer}}{aN}\frac{1}{[lipid]} \quad (6)$$

$$K_{app} = \frac{K_a^{bilayer}}{aN[\mathbf{L}]}\chi_L \quad (7)$$

In our titration experiments to check the validity of the Equations (6) and (7), the equilibrium constant was evaluated from the half-equivalence of the titration, that is, the point at which half of the ligand **L** was consumed to form $Eu\mathbf{L}_2$ [Eq. (8)]. The Eu concentration $[Eu]^{1/2equiv}$ required to complex half of the total amount of ligand **L** was taken as the value corresponding to a normalized fluorescence of $Eu\mathbf{L}_2$ of 0.5.

$$[\mathbf{L}]^{1/2equiv} = \frac{[\mathbf{L}]}{2} \text{ and } [EuL_2]^{1/2equiv} = \frac{[\mathbf{L}]}{4} \text{ then } K_{app} = \frac{1}{[Eu]^{1/2equiv}[\mathbf{L}]} \quad (8)$$

In a first experiment, titrations of LUVs containing 1 mol% or 2 mol% of ligand **L** with Eu^{III} were performed while maintaining constant [lipid], the total concentration of lipid. The two curves are nearly superimposed (Figure 6a), in agreement with Equation (6). If complexation occurred in solution, the curves would not be superimposed, since twice $[Eu]^{1/2equiv}$ is required to keep K_{app} constant [see Eq. (8)].

In a second experiment, titrations of **L**/EPC LUVs containing various molar percentages of **L** χ_L were performed while keeping constant [**L**], the total concentration of ligand **L**. The titration curves (Figure 6b) show the dependence on χ_L in vesicles. The apparent constant K_{app} was found to be proportional to χ_L (Figure 6c), as expected from Equation (7). If the reaction occurred in bulk, no change in the titration curves would be observed, since [**L**] was constant [see Eq. (8)]. The observed sigmoidal shape of the titration

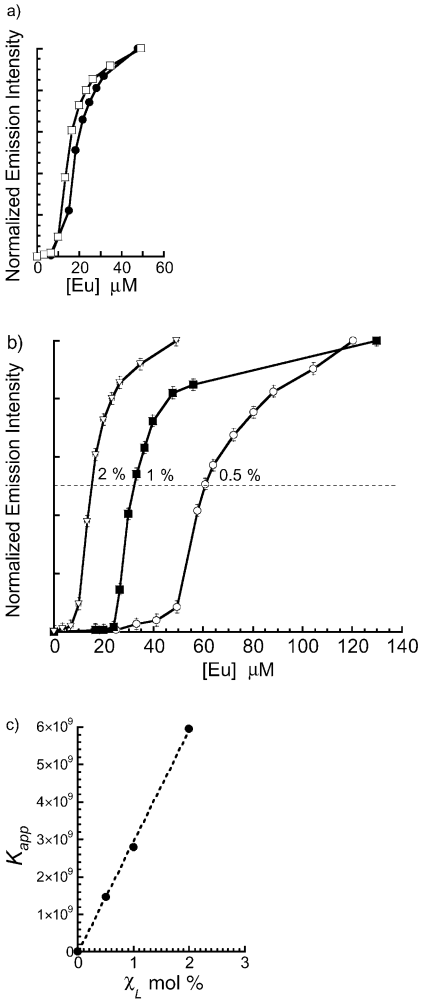

Figure 6. a) Variation of the emission intensity at 612 nm (excitation at 350 nm) of **L**/EPC LUVs with various molar fractions of **L** (χ_L) during titration by Eu: 1% (●), 2% (□). The total lipid concentration was fixed at [lipid] = 0.56 mM. b) Variation of the emission intensity at 612 nm (excitation at 350 nm) of LUVs with various molar fractions of **L** (χ_L) during titration with Eu: 0.5% (○), 1% (■), 2% (▽). The volume concentration of **L** was fixed at 11.2 μM. c) Corresponding evolution of the apparent constant K_{app} with χ_L

curves may be attributed to the formation of a complex with **L** or EPC. In particular, our Job titration in solution (see above) showed that the 1/1 complex Eu**L** was nonluminescent. The binding constant of Eu to EPC lipid, known to be in the range of 10^3–$10^4\ M^{-1}$, can be neglected in a first approximation in comparison to the binding of europium to the β-diketone ligand.[22]

In conclusion, the observed dependence of the apparent binding constant on the molar fraction of ligand **L** and on the lipid concentration confirms the 1/2 stoichiometry of the complex resulting from the binding of two ligands to Eu^{III} that occurs at the vesicle interface and is in agreement with the fact that the free ligand **L** and the complex $Eu\mathbf{L}_2$ are miscible in the membrane at these molar percentages of ligand **L** in the bilayer. The fraction of ligand **L** in the membrane appears to be a crucial parameter that shifts the equilibrium of complexation. The higher the concentration of the ligand in the membrane is, the higher the apparent equi-

librium constant for binding to the vesicle interface. Similar ligand cooperativity at the interface of membrane surface was recently observed.[27] Thus, the increase in ligand concentration leads in effect to the generation of a more powerful complexation site at the vesicle interface.[28] This property could explain why the affinity of a substrate for a membrane receptor can be reinforced by clustering of the receptors in biological membranes without changing the total number of receptors in the bilayer.[29] In biological systems, similar results were observed,[30] for example, in the association of pentameric cholera toxin with GM1, an oligosaccharide portion of the GM1 ganglioside. The binding of the toxin to the surface of a cell that is densely covered with GM1 moities occurs essentially irreversibly and with greater ΔG of association than the binding of five monomeric units of GM1.[31]

Eu^{III} ion transport across the membrane of the vesicles: Interestingly, no further increase in the emission intensity of $Eu\mathbf{L}_2$ was observed by addition at the end of the titration of an excess of cholate detergent, known to permeabilize and disrupt the vesicle bilayer. Therefore, one can conclude that the complexation at the interface of the vesicles engaged all the ligands of the membrane even if they were statistically distributed over the two leaflets initially. Since EPC lipid membranes are not permeable to lanthanides, the question arose how lanthanide ions are transported across the vesicle bilayer.

To address this question, a permeability test was developed. The strong competitor ligand DPA was encapsulated in **L**/EPC vesicles at a concentration of 30 mM so that DPA was in excess compared to the ligand **L** embedded in the vesicle membrane. $Eu(NO_3)_3$ was then added in excess. In solution, at the same concentrations of Eu^{III} and DPA, we observed the formation of the $Eu(DPA)_3$ complex, but the kinetics were too fast to be followed. In the case of **L**/EPC vesicles, the formation of the $Eu(DPA)_3$ and the $Eu\mathbf{L}_2$ complexes was followed by means of the variation of the emission intensity of Eu^{III} under excitation of DPA at 290 nm and of β-diketone **L** at 350 nm (Figure 7). The emission intensities of the $Eu(DPA)_3$ and $Eu\mathbf{L}_2$ complexes increased strongly up to a maximum and then slowly decreased. By comparison, no significant change in fluorescence occurred in the case of pure EPC vesicles (i.e., without ligand **L**) for excitation of DPA at 290 nm, that is, no $Eu(DPA)_3$ complex was formed. The very small change observed can be attributed to the slow release of DPA from the vesicles. These results clearly show that Eu^{III} ions were transported across the bilayer in the presence of the ligand **L**, and this process was followed by formation of the $Eu(DPA)_3$ complex.

The curve corresponding to the formation of $Eu(DPA)_3$ (Figure 7a) was fitted by a monoexponential function. The characteristic time τ for the formation of $Eu(DPA)_3$ was found to be around 15 s. This value is much higher than that observed in a DPA solution. This discrepancy suggests that DPA was not released into the external medium through membrane defects created by the ligand **L**, but that Eu^{III} ions passed through the membrane due to the dissociation of $Eu\mathbf{L}_2$ by DPA.

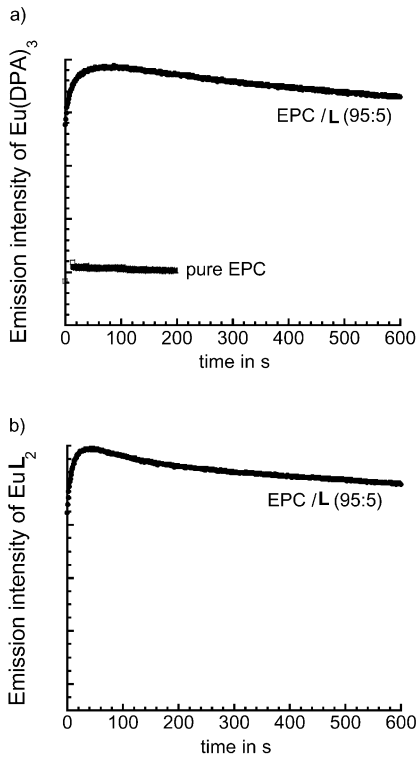

Figure 7. Evolution with time of the emission intensity induced by the addition of an excess of $Eu(NO_3)_3$ (33 μM) to a solution of vesicles ([Lipid] = 0.28 mM) containing 30 mM DPA: a) by excitation at 290 nm ($Eu(DPA)_3$), b) by excitation at 350 nm ($Eu\mathbf{L}_2$)

Two kinds of mechanisms can be envisaged for ion transport: 1) transverse movement (flip-flop) of the complexed ligand and 2) formation of pores consecutive to complexation of **L**, which can induce ligand clustering. The observed transport kinetics are rather fast ($\tau = 15$ s) compared to the usual transport by a flip-flop mechanism ($\tau = 1$–30 min)[26] and therefore tend to exclude such a mechanism.

To obtain further information on the transport mechanism, the effect of membrane fluidity on the permeability to lanthanides was tested. Matrix rigidity is expected to slow down dramatically the kinetics of the transport by flip-flop movement because of restriction of lipid motion. Therefore, dipalmitoyl phosphatidylcholine (DPPC), which exists in a gel phase below 41 °C, was used as lipid matrix. The **L**/DPPC (5/95) vesicles containing DPA at a concentration of 30 mM were titrated with Eu^{III} at room temperature. The characteristic time for the formation of $Eu(DPA)_3$, found to be 35 s, is comparable to that obtained for a fluid EPC lipid matrix (15 s). Consequently, the rigidity of the membrane does not significantly change the kinetics of formation of $Eu(DPA)_3$ and those of Eu^{III} transport. This result speaks against flip-flop as the main mechanism of transport. Nevertheless, our experiments do not permit the mechanism to be elucidated completely. The complexation of the ligand **L** could either facilitate the opening of pores due to a possible reorientation of the ligands **L** in the membrane once they are complexed, or the formation of the complex could induce defects in the membrane by clustering of ligands, which could increase the permeability of the membrane and

permit the passage of Eu^{III}. Similar effects on vesicle permeability were already attributed to the reorientation of the carrier molecule in the case of an amphiphilic peptide.[32] In conclusion these experiments show clearly that europium ions are transported across the membrane due to the presence of the ligand **L** but do not elucidate by which mechanism this transport occurs.

To define the role of the amphiphilic ligand **L** in the ion transport, kinetics experiments were performed at various pH values and at various molar fractions χ_L of the amphiphilic ligand **L** (Table 2).

First, the characteristic time values τ decreased with increasing pH, as expected from the acid/base properties of the β-diketone ligand **L**. At basic pH the β-diketone group is partially deprotonated. The pK_a values of acetylacetone in water and DMSO are 8.9 and 13.3, respectively, while the pK_a of dibenzoylmethane in DMSO is 13.35.[33] By analogy the pK_a of β-diketone ligand **L** in water was assumed to be around 9. The presence of small clusters of **L** in EPC membrane, suggested by the DSC measurements, could explain why the kinetics are faster for 5 mol% than for 1 mol% of **L**. These results show that the amphiphilic ligand **L** induces the transport of Eu^{III} across the vesicle membrane by complexation and that the kinetics can be modulated by the surface concentration of the ligand **L** and also by the pH of the medium.

Table 2. Effect of the molar fraction of **L** χ_L and pH on the kinetics of permeation of Eu^{III} into **L**/EPC vesicles containing a 30 mM DPA solution, evaluated by a monoexponential fit of the kinetic curves of DPA/Eu^{III} complexation.

χ_L	pH	$\tau \pm 10\%$ [s]
5	8	15
1	9	116
1	8	143
1	7	208

Conclusion

The results described here show that incorporation of a synthetic amphiphilic β-diketone ligand **L** in a vesicular membrane allows a tunable control of the permeability of the membrane to Eu^{III} ions. The ion/β-diketone ligand molecular recognition occurs by reversible complexation at the surface of the vesicle and results in selective and fast transport of lanthanide ions across the vesicle membrane assisted by the amphiphilic β-diketone ligand, as shown in Figure 8.

The observed complexation involves two ligands of the same vesicle membrane (intravesicular complexation). This synthetic system shows a very interesting synergic effect in which the binding constant at the vesicle interface is modulated by the ligand concentration in the membrane. This system offers an example of the design of artificial functional vesicular systems that can selectively transport ions. For a better understanding of the actual mechanism of transport, it would be necessary to elucidate the orientation of the ligand within the membrane and its possible reorientation following its complexation.

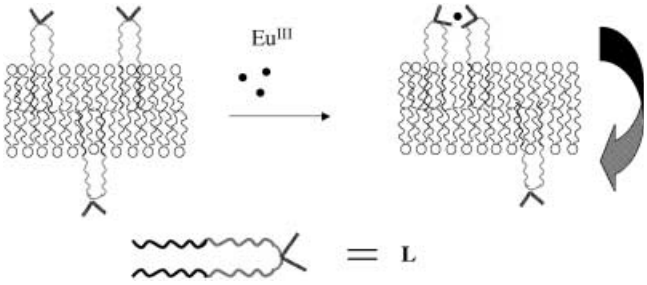

Figure 8. Schematic mechanism of the complexation at the surface of vesicles and ion transport across the vesicle membrane assisted by the diketone ligand **L**

The next step towards the self-assembly of vesicles by metal/ligand interaction is to explore how to induce the formation of a complex between two different vesicles (intervesicular complexation), which is a key step towards a selective self-assembly of vesicles into organized polyvesicular architectures.

Experimental Section

Synthesis of the ligands

General: IR: Perkin-Elmer 297, KBr pellets. NMR ($CDCl_3$): Bruker AM200SY equipped with Aspect 3000 data system, δ in ppm downfield from TMS, J in Hz. TLC: Merck, silica gel 60 F254, 0.25 mm (analytical TLC), UV detection. Preparative column chromatography: Merck silica gel 60 (0.040–0.063 mm). Elemental analyses: Service Central d'Analyse du CNRS. M.p. and enthalpies of fusion (ΔH): Perkin-Elmer DSC7 differential scanning calorimeter, heating or cooling rate 5 °C min^{-1} unless otherwise stated, temperatures in °C, ΔH in kJ mol^{-1}. As usual, the presence of mesophases was detected when the phase transitions did not exhibit significant hysteresis in the cooling runs. The very low enthalpies of the two transitions between 1 and −25 °C could be associated with rotator phases similar to those displayed by long-chain linear alkanes.[34] Complete characterization of the observed mesophases would require more thorough studies beyond the scope of the present paper.

Tetraethyleneglycol monohexadecyl ether *p*-toluenesulfonate (2a): Tosyl chloride (2.3 g, 12 mmol) was added with stirring to an ice-cooled solution of commercial tetraethyleneglycol monohexadecyl ether (**1a**, 3.3 g, 7.9 mmol) in dry pyridine (15 mL). The reaction mixture was kept at 4 °C for 22 h and poured into ice water (ca. 40 mL). The mixture was extracted with diethyl ether (2 × 40 mL) and the organic phases washed with 1N HCl (4 × 10 mL) and brine. Drying over Na_2SO_4 and evaporation afforded **2a** (4.0 g, 88%), which was used for the next step without further purification ^{1}H NMR: $\delta = 7.80$ (d, $J = 8$ Hz, 2H), 7.34 (d, $J = 8$ Hz, 2H), 4.16 (t, 2H), 3.58–3.66 (m, 14H), 3.44 (t, $J = 7$ Hz, 2H), 2.45 (s, 3H), 1.57 (m, 2H), 1.25 (m, 26H), 0.88 ppm (t, 3H).

Hexaethyleneglycol mono hexadecyl ether *p*-toluenesulfonate (2b): Prepared by the same procedure described for **2a**, from commercial hexaethyleneglycol monohexadecyl ether (**1b**, 3.04 g, 6 mmol) and tosyl chloride (2.3 g, 12 mmol) in dry pyridine (15 mL). The crude product **2b** (3.06 g, 91%) was used for the next step without further purification ^{1}H NMR: $\delta = 7.78$ (d, $J = 8$ Hz, 2H), 7.32 (d, $J = 8$ Hz, 2H), 4.14 (t, 2H), 3.56–3.69 (m, 22H), 3.42 (t, $J = 7$ Hz, 2H), 2.43 (s, 3H), 1.55 (m, 2H), 1.24 (m, 26H), 0.86 ppm (t, 3H).

3-[hexadecyloxy(tetraethyleneoxy)]acetophenone (3a): A mixture of 3-hydroxyacetophenone (210 mg, 1.5 mmol), **2a** (0.86 g, 1.5 mmol), and dry K_2CO_3 (0.75 g, 5.4 mmol) in dry DMF (7.5 mL) was stirred at 80 °C for 24 h under nitrogen. The mixture was poured into ice water (ca. 30 mL) and extracted with diethyl ether (2 × 30 mL). The organic extracts were

washed with water (3×10 mL), dried over Na_2SO_4, and concentrated. The residue (780 mg) was subjected to chromatography (silica gel, 40 g, elution with AcOEt/hexane 20/80) to provide **3a** (710 mg, 88%), which was recrystallized from pentane at 0°C for analysis. DSC (M = metastable mesophase): K→I 33°C, $\Delta H = 105\ kJ\,mol^{-1}$ (1st heating run); I→M 17.5°C, $\Delta H = 42\ kJ\,mol^{-1}$, M→M −0.2°C, $\Delta H = 0.8\ kJ\,mol^{-1}$, M→M −23°C, $\Delta H = 1.5\ kJ\,mol^{-1}$ (1st cooling run); M→M −22.5°C, $\Delta H = 1.7\ kJ\,mol^{-1}$, M→M 1°C, $\Delta H = 0.75\ kJ\,mol^{-1}$; M→K ca. 5–10°C (exothermic crystallization), K→I 32°C, $\Delta H = 103\ kJ\,mol^{-1}$ (2nd heating run). Recrystallization could be avoided when cooling was stopped at 10°C and heating proceeded immediately thereafter: M→M 18.8°C, $\Delta H = 42\ kJ\,mol^{-1}$. ^1H NMR: $\delta = 7.49$–7.56 (m, 2H), 7.36 (t, $J = 8$ Hz, 1H), 7.10–7.16 (m, 1H), 4.18 (m, 2H), 3.88 (m, 2H), 3.56–3.75 (m, 12H), 3.43 (t, $J = 7$ Hz, 2H), 2.59 (s, 3H), 1.57 (m, 2H), 1.25 (m, 26H), 0.88 ppm (t, 3H); elemental analysis (%) calcd for $C_{32}H_{56}O_6$ (536.78): C 71.60, H 10.52; found: C 71.52, H 10.62.

3-[hexadecyloxy(hexaethyleneoxy)]acetophenone (3b): Prepared by the same procedure described for **3a** from 3-hydroxyacetophenone (275 mg, 2 mmol), **2b** (1.32 g, 2 mmol), and dry K_2CO_3 (1 g, 7.25 mmol) in dry DMF (10 mL). The crude product (1.25 g) was subjected to chromatography (silica gel, 50 g, elution with AcOEt/hexane 70/30) to give **3b** (990 mg, 80%). DSC: K→K ca. 20°C, K→I 27–30°C (several ill-resolved peaks), $\Delta H = 113\ kJ\,mol^{-1}$ (1st heating run); I→M 14.7°C, $\Delta H = 44\ kJ\,mol^{-1}$, M→M −1.3°C, $\Delta H = 0.74\ kJ\,mol^{-1}$, M→M −23.8°C, $\Delta H = 1.5\ kJ\,mol^{-1}$ (1st cooling run); M→M −23.6°C, $\Delta H = 1.6\ kJ\,mol^{-1}$, M→M −0.2°C, $\Delta H = 0.76\ kJ\,mol^{-1}$, M→I 16°C, $\Delta H = 44\ kJ\,mol^{-1}$ (2nd heating run). Contrary to **3a**, no recrystallization was observed. ^1H NMR: $\delta = 7.47$–7.54 (m, 2H), 7.34 (t, $J = 8$ Hz, 1H), 7.08–7.14 (m, 1H), 4.16 (m, 2H), 3.86 (m, 2H), 3.54–3.74 (m, 20H), 3.42 (t, $J = 7$ Hz, 2H), 2.57 (s, 3H), 1.55 (m, 2H), 1.23 (m, 26H), 0.86 ppm (t, 3H); elemental analysis (%) calcd for $C_{36}H_{64}O_8$ (624.89): C 69.19, H 10.32; found: C 69.13, H 10.44.

Ethyl 3-[hexadecyloxy(tetraethyleneoxy)]benzoate (4a): A mixture of ethyl 3-hydroxybenzoate (300 mg, 1.8 mmol), **2a** (1.03 g, 1.8 mmol), and dry K_2CO_3 (0.9 g, 6.5 mmol) in dry DMF (9 mL) was stirred at 80°C for 24 h under nitrogen. The mixture was poured into ice water (ca. 30 mL) and extracted with diethyl ether (2×30 mL). The organic extracts were washed with water (3×10 mL), dried over Na_2SO_4, and concentrated. The residue (980 mg) was subjected to chromatography twice (silica gel, 45 g and 20 g, elution with AcOEt/hexane 40/60) to provide **4a** (750 mg, 73%), which was recrystallized from MeOH/pentane for analysis. DSC: K→I 27–28°C (2 ill-resolved peaks), $\Delta H = 103\ kJ\,mol^{-1}$ (1st heating run); I→M 10.3°C, $\Delta H = 42\ kJ\,mol^{-1}$, M→M −0.8°C, $\Delta H = 0.7\ kJ\,mol^{-1}$ (1st cooling run stopped at −10°C); M→M 0.4°C, $\Delta H = 0.6\ kJ\,mol^{-1}$, M→I 11.6°C, $\Delta H = 42\ kJ\,mol^{-1}$ (2nd heating run), no recrystallization was observed. ^1H NMR: $\delta = 7.56$–7.66 (m, 2H), 7.33 (t, $J = 8$ Hz, 1H), 7.09–7.14 (m, 1H), 4.36 (q, $J = 7$ Hz, 2H), 4.17 (m, 2H), 3.87 (m, 2H), 3.55–3.75 (m, 12H), 3.43 (t, $J = 7$ Hz, 2H), 1.56 (m, 2H), 1.39 (t, $J = 7$ Hz, 3H), 1.25 (m, 26H), 0.88 ppm (t, 3H); elemental analysis (%) calcd for $C_{33}H_{58}O_7$ (566.81): C 69.93, H 10.31; found: C 69.93, H 10.33.

Ethyl 3-[hexadecyloxy(hexaethyleneoxy)]benzoate (4b): Prepared by the same procedure described for **4a**, from ethyl 3-hydroxybenzoate (330 mg, 2 mmol), **2b** (1.32 g, 2 mmol), and dry K_2CO_3 (1 g, 7.25 mmol) in dry DMF (10 mL). The crude product (1.27 g) was subjected to chromatography (silica gel, 50 g, elution with AcOEt/hexane 70/30) to give **4b** (1.04 g, 79%) as a liquid. DSC at 5°C min^{-1}: I→M 7.8°C, $\Delta H = 42\ kJ\,mol^{-1}$, M→M −2.2°C, $\Delta H = 0.75\ kJ\,mol^{-1}$, M→M −24.6°C, $\Delta H = 1.8\ kJ\,mol^{-1}$ (cooling run); M→M −24.5°C, $\Delta H = 1.9\ kJ\,mol^{-1}$, M→M −1.5°C, $\Delta H = 0.75\ kJ\,mol^{-1}$, M→M→K 8°C with partial simultaneous crystallization starting at 5°C, K→I ≈11–13°C (2 melting peaks, heating run). DSC at 1°C min^{-1}: recrystallization could be avoided when cooling was stopped at 5°C and heating proceeded immediately thereafter: M→M 8°C, $\Delta H = 41\ kJ\,mol^{-1}$. ^1H NMR: $\delta = 7.55$–7.64 (m, 2H), 7.31 (t, $J = 8$ Hz, 1H), 7.07–7.12 (m, 1H), 4.35 (q, $J = 7$ Hz, 2H), 4.16 (m, 2H), 3.85 (m, 2H), 3.53–3.73 (m, 20H), 3.42 (t, $J = 7$ Hz, 2H), 1.55 (m, 2H), 1.39 (t, $J = 7$ Hz, 3H), 1.24 (m, 26H), 0.86 ppm (t, 3H); elemental analysis (%) calcd for $C_{37}H_{66}O_9$ (654.91): C 67.86, H 10.16; found: C 67.86, H 10.16.

Diketone 5a (L): 1,2-Dimethoxyethane (DME, 20 mL), **3a** (537 mg, 1 mmol), and **4a** (567 mg, 1 mmol) were added to NaH (120 mg of 60% suspension in oil, 3 mmol) that had been washed three times with dry pentane by decantation. The reaction mixture was stirred and heated to reflux for 12 h under nitrogen. After cooling and addition of two drops of water, the mixture was poured into ice water (20 mL) and 1N HCl (10 mL). The resulting crystals were collected by filtration, washed with water, and dried at room temperature. This crude product (1.06 g) was subjected to chromatography (silica gel, 50 g, elution with AcOEt/hexane 40/60, then AcOEt) and recrystallized from CH_2Cl_2/MeOH at 0°C to give **5a** (345 mg, 33%). DSC: K→K ≈60°C, K→I 65–68°C (several ill-resolved peaks), $\Delta H = 172\ kJ\,mol^{-1}$, (no mesophase). ^1H NMR: $\delta = 7.53$–7.58 (m, 4H), 7.34 (t, $J = 8$ Hz, 2H), 7.09–7.14 (m, 2H), 6.81 (s, 1H), 4.22 (m, 4H), 3.90 (m, 4H), 3.55–3.75 (m, 24H), 3.43 (t, $J = 7$ Hz, 4H), 1.57 (m, 4H), 1.25 (m, 52H), 0.88 ppm (t, 6H); elemental analysis (%) calcd for $C_{63}H_{108}O_{12}$ (1057.52): C 71.55, H 10.30; found: C 71.53, H 10.35.

Diketone 5b: Prepared by the procedure described for **5a**, from **3b** (312 mg, 0.5 mmol), **4b** (327 mg, 0.5 mmol), and NaH (60 mg of 60% suspensionin oil, 1.5 mmol) in DME (10 mL). The crude product (610 mg) was subjected to chromatography (silica gel, 60 g, elution with AcOEt/MeOH 96/4) and recrystallized twice from CH_2Cl_2/MeOH to afford **5b** (118 mg, 19%). DSC: K→I 57–58.5°C (2 ill-resolved peaks), $\Delta H = 216\ kJ\,mol^{-1}$ (1st heating run); I→M 18.8°C, $\Delta H = 77\ kJ\,mol^{-1}$ (cooling runs); M→I ≈20°C, $\Delta H = \approx 75\ kJ\,mol^{-1}$, exothermic recrystallization occurring just after I→K 22–30°C, $\Delta H = \approx 155\ kJ\,mol^{-1}$, exothermic K→K 47°C, $\Delta H = 25\ kJ\,mol^{-1}$, K→I 58°C, $\Delta H = 210\ kJ\,mol^{-1}$ (next heating runs). ^1H NMR: $\delta = 7.45$–7.50 (m, 4H), 7.30 (t, $J = 8$ Hz, 2H), 7.01–7.07 (m, 2H), 6.74 (s, 1H), 4.14 (m, 4H), 3.82 (m, 4H), 3.50–3.65 (m, 40H), 3.35 (t, $J = 7$ Hz, 4H), 1.49 (m, 4H), 1.27 (m, 52H), 0.88 ppm (t, 6H); elemental analysis (%) calcd for $C_{71}H_{124}O_{16}$ (1233.73): C 69.12, H 10.13; found: C 69.10, H 10.16.

Vesicle preparation and characterization

LUV preparation by extrusion: LUVs were prepared according to standard procedures.[35] A lipid film was formed by evaporation of a chloroform solution of the lipid mixture (13 μmol) in a 10 mL round-bottomed flask under reduced pressure at room temperature. The lipid film was then hydrated with the appropriate aqueous buffer or water (1 mL) and subjected to five freeze–thaw cycles with liquid nitrogen and water at 20°C. The obtained lipid suspension was then extruded ten times through a Whatman laser-etched polycarbonate membrane with 100 nm pore size at 40°C. Purification was performed by gel exclusion on a prepacked Sephadex G-10 column (Pharmacia) to give a final lipid concentration of 4.3 mM.

For the incorporation of DPA, the amount of DPA in the vesicle represents around three equivalents of **L** embedded in the vesicle membrane in the permeability experiment by assuming that the incorporation yield of **L** is around 100% during vesicle preparation and given a vesicle diameter of 100 nm.

Differential scanning calorimetry measurements on the suspension of multilamellar vesicles (MLVs): the suspension of MLVs composed of **L**:EPC and **L**:DPPC mixtures were prepared as follows: A lipid film was formed by evaporation of a chloroform solution of the lipid mixture (60 μmol) in a 5 mL round-bottomed flask under reduced pressure at room temperature. This lipid film was then hydrated with water (500 μL) and subjected to ten freeze–thaw cycles with liquid nitrogen and water at 20°C until the mixture was a homogeneous suspension. The total lipid concentration was around 100 mg mL^{-1}. These suspensions were weighed (50 mg) into a steel capsule. At least two heating/cooling cycles were performed at 5°C min^{-1}.

UV and fluorescence spectroscopy: A DU 640 Beckman UV spectrometer was used for UV absorbance measurements. The excess absorbance calculated for the Job titration was calculated according to the following relation: $A_{exc}(x) = A(x) - [[A(1) - A(0)]x + A(0)]$ where $A(x)$ is the absorbance of the solution containing a molar fraction x of **L**. Titrations of vesicles were performed by fluorescence spectroscopy at room temperature by using a SPEX FluoroMax spectrometer at a constant volume of 3 mL.

Freeze-fracture transmission electron microscopy: To achieve the best preservation of the sample structure on cryofixation, we replaced water with water/glycerol (33 vol%) solution. A 20–30 μm thick layer of the sample was deposited on a thin copper holder and then rapidly quenched in liquid propane. The frozen samples were fractured in vacuo (ca. 10^{-7} Torr) with the liquid-nitrogen-cooled knife of a Balzers 301 freeze-etching unit. The replication was performed by unidirectional shadowing with platinum/carbon at an angle of 35°. The mean thickness of the metal

deposit was 1–1.5 nm. The replicas were washed with organic solvents and distilled water and then observed under a Philips EM 410 electron microscope. The contrast of images is related to the depth fluctuations of the metal deposit.

Light scattering measurements: Vesicle samples were filtered through Nucleopore filters (pore size: 0.25 μm) at 0.1–0.5 mM lipid concentration. The dynamic light scattering measurements were carried out on a 4700/PCS100 (Malvern) at several angles. A coherent argon laser at 514.5 nm produced incident irradiation. Correlation functions were analyzed by the method of cumulants to give the hydrodynamic diameters. The error indicated for the mean diameter was estimated from the half-width of the size-distribution peak.

Acknowledgement

We thank Hubert Hervet for helpful discussions concerning the light scattering measurements and Franck Artzner for his suggestions concerning the DSC measurements.

[1] D. E. Green, M. Fry, G. A. Blondin, *Proc. Natl. Acad. Sci. USA* **1980**, *77*, 257–261.
[2] D. W. Deamer, J. Bramhall, *Chem. Phys. Lipids* **1986**, *40*, 167.
[3] K. Binnemans, C. Görller-Walrand, *Chem. Rev.* **2002**, *102*, 2303–2345.
[4] F. Hwang, D. Q. Zhao, J. W. Chen, X. H. Chen, J. Z. Ni, *Chem. Phys. Lipids* **1996**, *82*, 73.
[5] G. Cevc, H. Richardsen, *Adv. Drug Delivery Rev.* **1999**, *38*, 197–232.
[6] P. Scrimin, P. Tecilla, R. A. Moss,, K Braken, *J. Am. Chem. Soc.* **1998**, *120*, 1179–1185.
[7] J. Bentz, D. Alford, J. Cohen, N. Düzgünes, *Biophys. J.* **1988**, *53*, 593–607.
[8] F. S. Richardson, *Chem. Rev.* **1982**, *82*, 541–552.
[9] J.-M. Lehn, *PNAS* **2002**, *99*, 4763–4768.
[10] C. M. Paleos, Z. Sideratou, D. Tsiourvas, *ChemBioChem* **2001**, *2*, 305–310.
[11] V. Marchi-Artzner, T. Gulik-Krzywicki, M.-A. Guedeau-Boudeville, C. Gosse, J. Sanderson, J.-C. Dedieu, J.-M. Lehn, *ChemPhysChem* **2001**, *2*, 367–376.
[12] P. Scrimin, P. Tecilla, *Curr. Opin. Chem. Biol.* **1999**, *3*, 730–735.
[13] J.-C. G. Bünzli, C. Piguet, *Chem. Rev.* **2002**, *102*, 1897–1928.
[14] A. Orellana, M.-L. Lankkanen, K. Keinänen, *Biochim. Biophys. Acta* **1996**, *1284*, 29–34.
[15] *Contrast Agents I, Magnetic Resonance Imaging* (Ed.: W. Krause), Springer, Berlin, **2002**.
[16] R. B. Lauffer, *Chem. Rev.* **1987**, *87*, 901–927.
[17] K. Ohta, A. Ishii, H. Muroki, I. Yamamoto, K. Matsuzaki, *Mol. Cryst. Liq. Cryst.* **1985**, *116*, 299–307.
[18] W. C. Vosburgh, G. Cooper, *J. Am. Chem. Soc.* **1941**, *63*, 437–442.
[19] H. Bauer, J. Blanc, D. L. Ross, *J. Am. Chem. Soc.* **1964**, *86*, 5125–5131.
[20] See for example N. Hauet, F. Artzner, F. Boucher, C. Grabielle-Madelmont, I. Cloutier, G. Keller, P. Lesieur, D. Durand, M. Paternostre, *Biophys. J.* **2003**, *84*, 3123–3137.
[21] J. Westman, L. E. G. Erickson, A. Ehrenberg, *Biophys. Chem.* **1984**, *19*, 57.
[22] R. Lehrmann, J. Seelig, *Biochim. Biophys. Acta* **1994**, *1189*, 89–95.
[23] F. Pincet, S. Cribier, E. Perez, *Eur. Phys. J. B* **1999**, *11*, 127–130.
[24] J. R. Lakowicz, G. Piszczek, B. P. Maliwal, I. Gryczynski, *ChemPhysChem* **2001**, *4*, 247–252.
[25] A. E. Martell, R. M. Smith, *Critical Stability Constants, Vol. 1*, *Amino Acids*, Plenum Press, New York, 1974.
[26] D. D. Lasic, *Liposomes: from Physics to Applications*, Elsevier, Amsterdam, **1993**.
[27] E. L. Doyle, C. A. Hunter, H. C. Phillips, S. J. Webb,, N. H. Williams, *J. Am. Chem. Soc.* **2003**, *125*, 4593–4599.
[28] M. Mammen, S.-K. Choi, G. M. Whitesides, *Angew. Chem.* **1998**, *110*, 2908–2953; *Angew.Chem. Int. Ed.* **1998**, *37*, 2754–2794.
[29] J. E. Gestwicki, L. E. Strong, L. L. Kiessling, *Chem.Biol.* **2000**, *7*, 583–591.
[30] M. Mammen, S.-K. Choi, G. M. Whitesides, *Angew. Chem.* **1998**, *110*, 2908; *Angew. Chem. Int. Ed.* **1998**, *37*, 2754–2794.
[31] A. Schoen, E. Freire, *Biochemistry* **1989**, *28*, 5019–5024.
[32] P. Scrimmin, P. Tecilla, U. Tonellato, A. Veronese, M. Crisma, F. Formaggio, C. Toniolo, *Chem. Eur. J.* **2002**, *8*, 2753–2763.
[33] F. G. Bordwell, *Acc. Chem. Res.* **1988**, *21*, 456–463.
[34] See for example: J. Doucet, I. Denicolo, A. Craievich, *J. Chem. Phys.* **1981**, *75*, 5125–5127; E. B. Sirota, D. M. Singer, *J. Chem. Phys.* **1994**, *101*, 10873–10882.
[35] G. Gregoriadis, *Liposomes Technology*, CRC, Boca Raton, FL, **1984**.

Received: August 1, 2003
Revised: December 23, 2003 [F5423]